Structural Characterization of Gangliosides and Glycolipids via Ultraviolet Photodissociation Mass Spectrometry

*John P. O'Brien and Jennifer S. Brodbelt**

Department of Chemistry and Biochemistry
The University of Texas at Austin
1 University Station A5300
Austin, TX, USA 78712

Correspondence to: Jennifer Brodbelt, jbrodbelt@cm.utexas.edu

Running title: Gangliosides via UVPD-MS

Supplemental materials include:

Structures of compounds.

CID, HCD and UVPD spectra of numerous gangliosides.

Tables of identified gangliosides

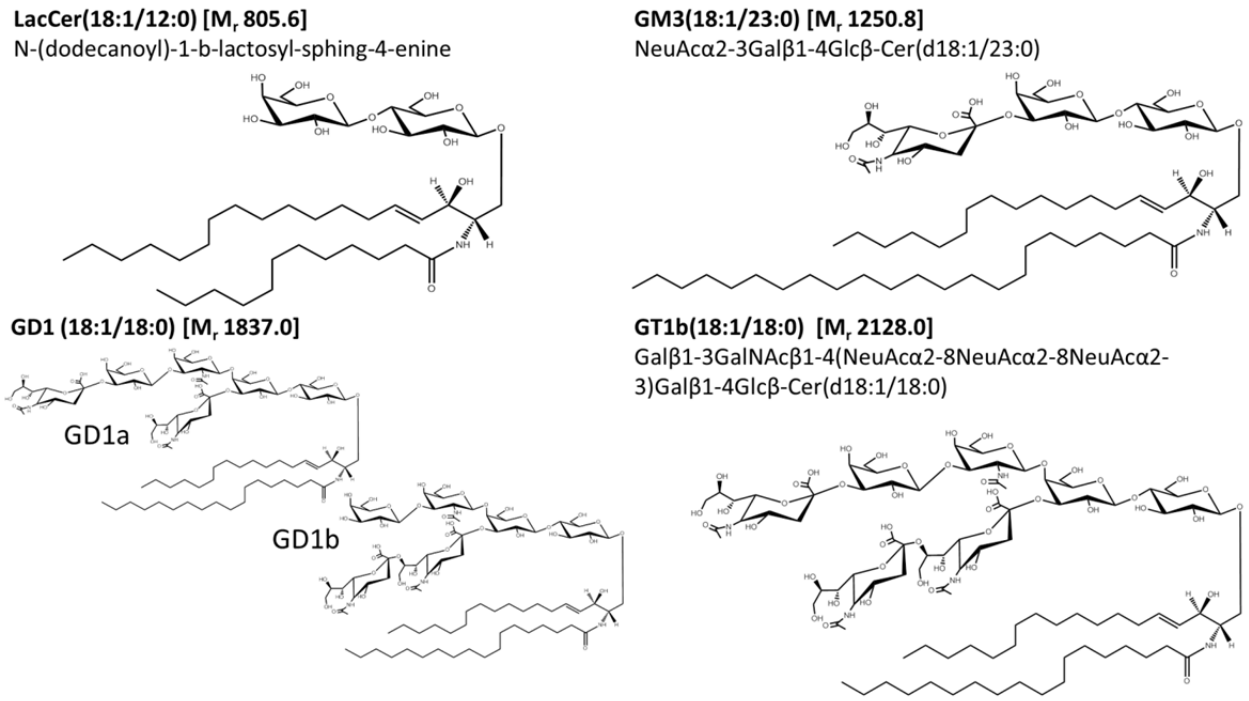

Supplemental Figure 1. Structures of gangliosides and glycosphingolipids. The ceramide structure is described in parenthesis by the total number of carbon atoms in sphingoid base chain and the number of double bonds in the chain, followed by the total number of carbon atoms in the fatty acid and number of double bonds in the chain. The monoisotopic molecular masses are shown in brackets.

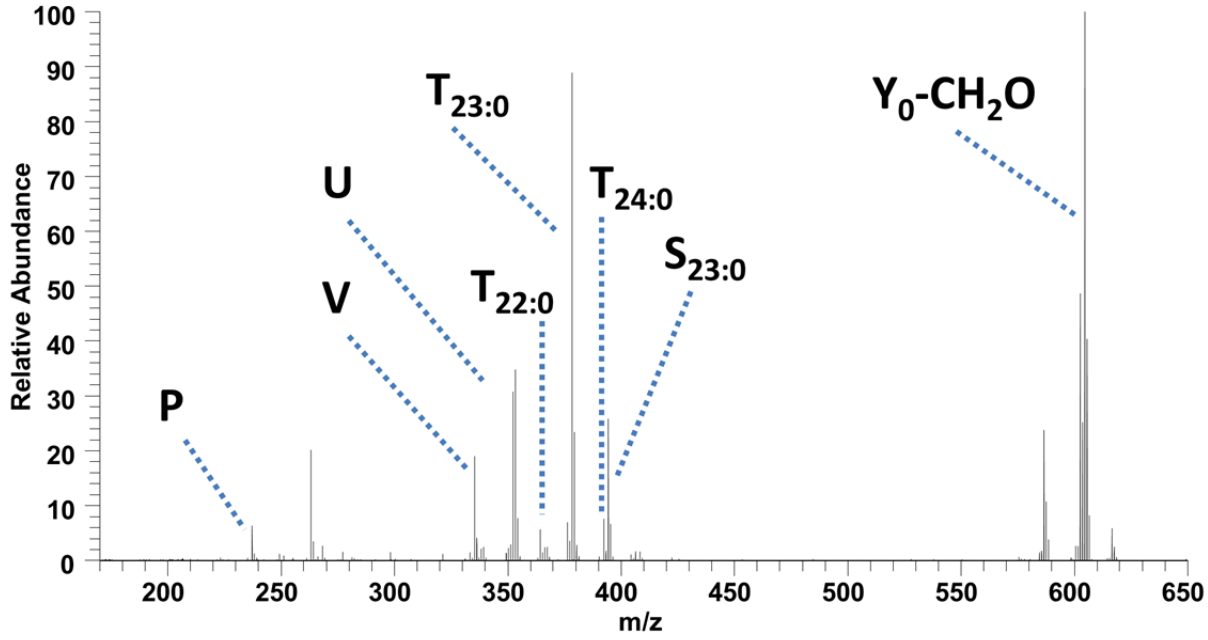

Supplemental Figure 2. CID-MS/MS/MS spectrum of GM3(18:1/23:0) Y_o fragment ion.

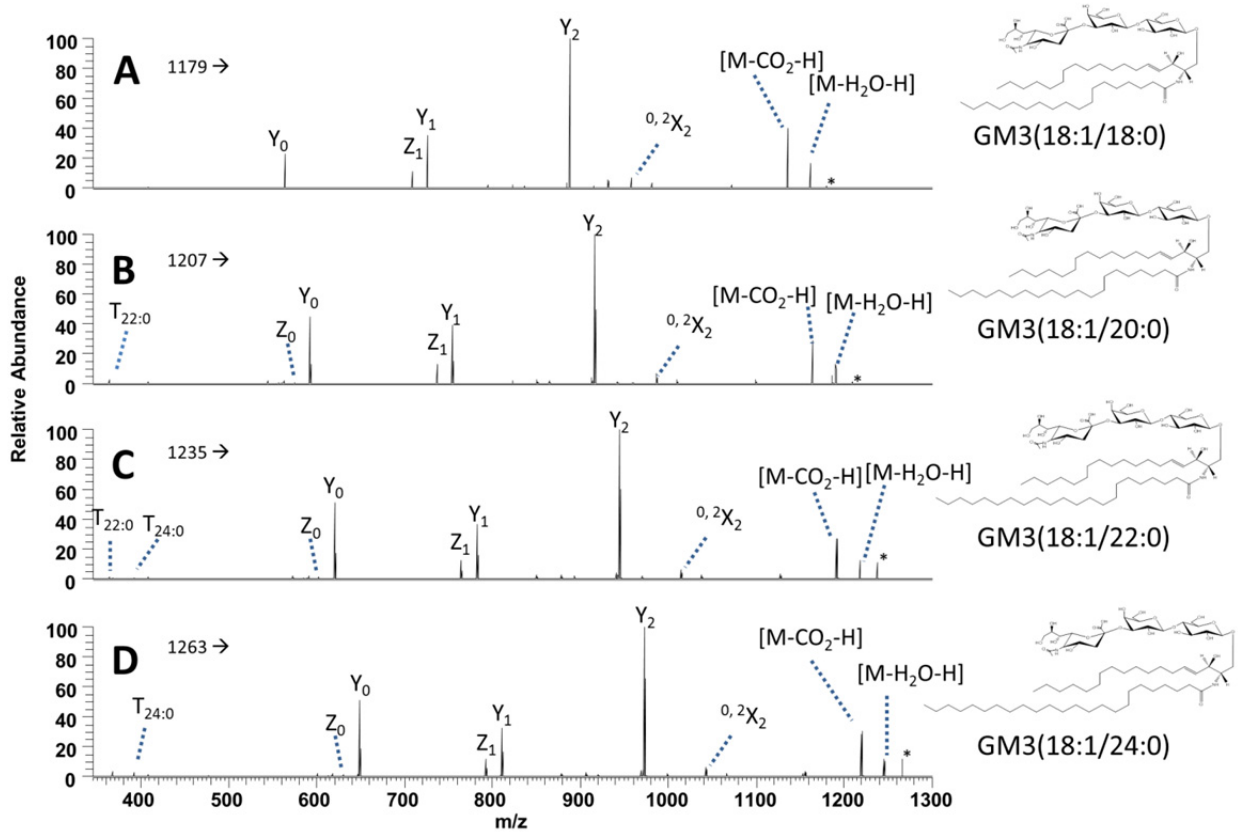

Supplemental Figure 3. CID mass spectra of singly deprotonated GM3 gangliosides with variable amide and sphingoid base lengths. The precursor ion is labelled with an asterisk.

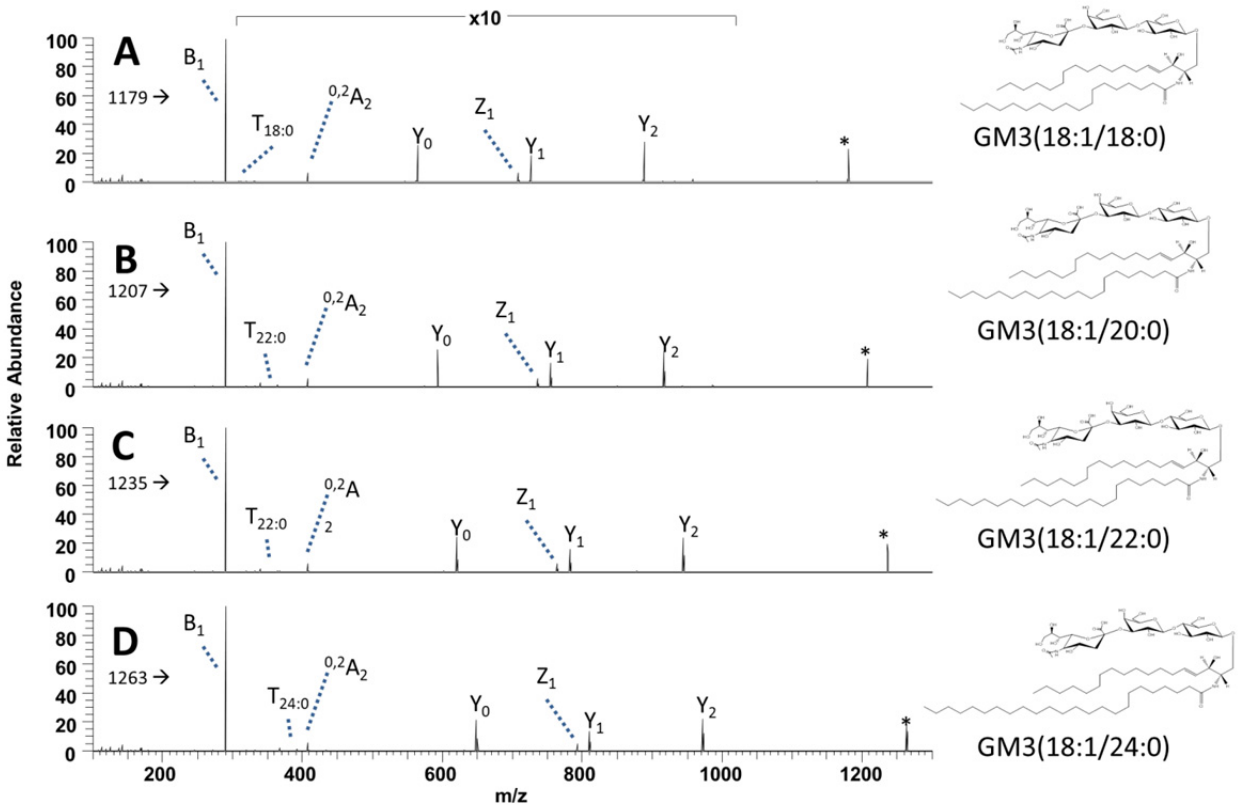

Supplemental Figure 4. HCD mass spectra of singly deprotonated GM3 gangliosides with variable amide and sphingoid base lengths. The precursor ion is labelled with an asterisk.

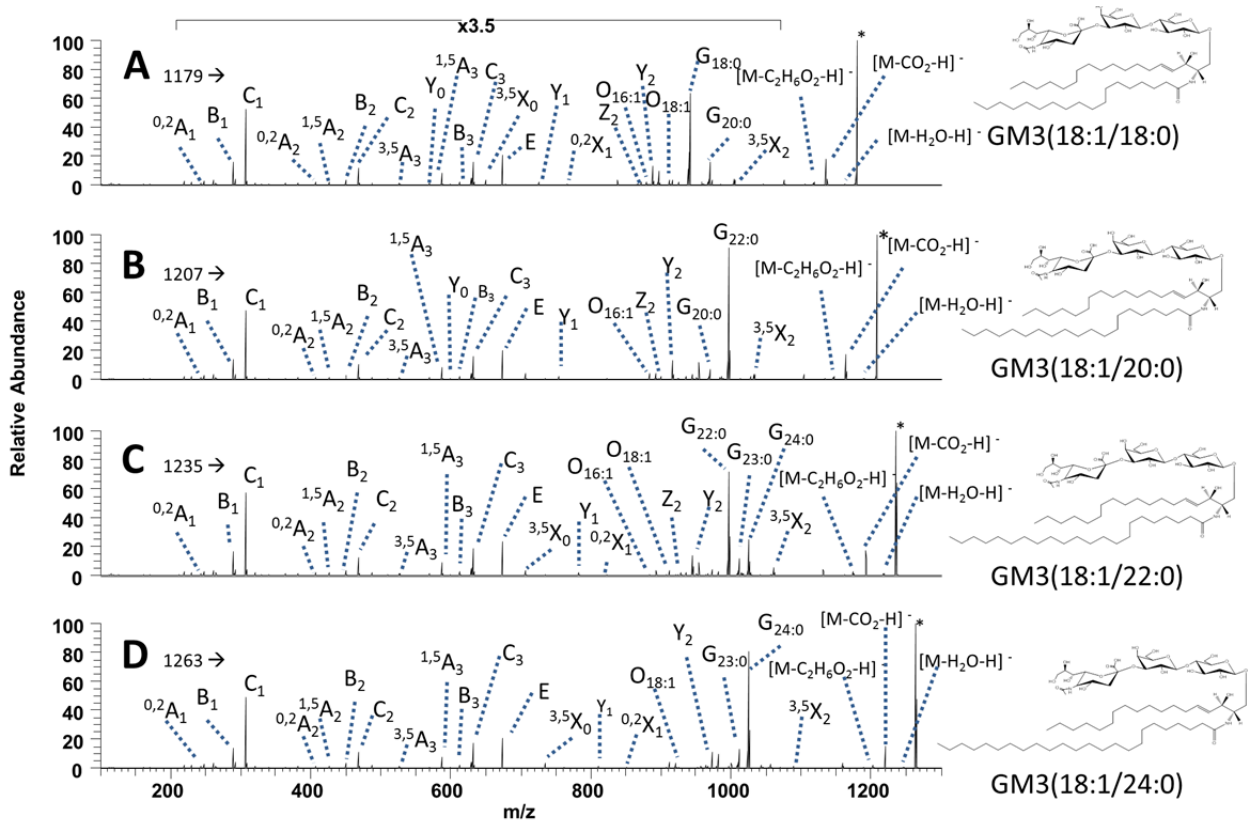

Supplemental Figure 5. UVPD mass spectra of singly deprotonated GM3 gangliosides with variable amide and sphingoid base lengths. The precursor ion is labelled with an asterisk.

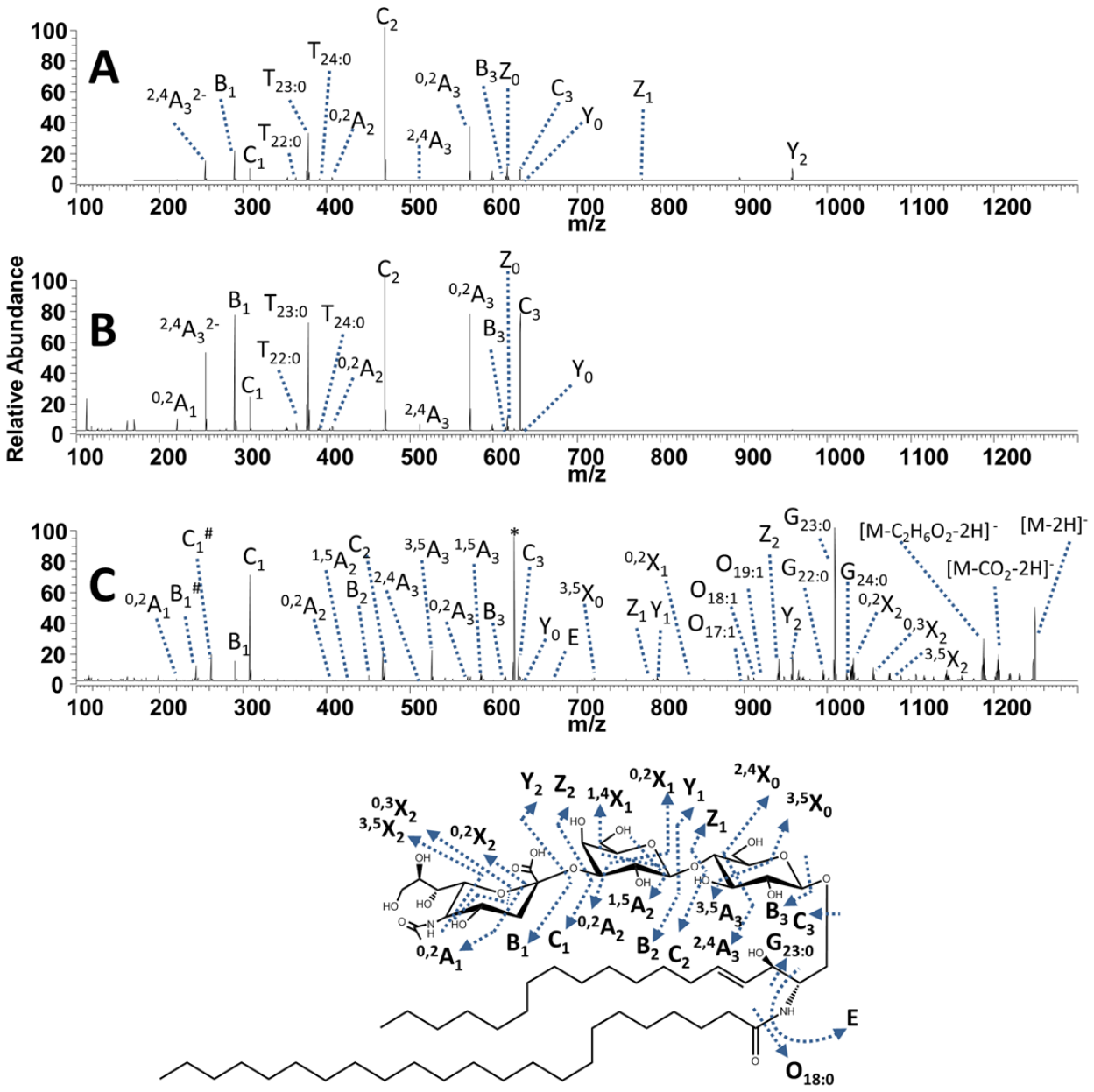

Supplemental Figure 6. (A) CID, (B) HCD and (C) UVPD mass spectra of the doubly deprotonated bovine milk ganglioside GM3(18:1/23:0). The precursor ion is labelled with an asterisk. Fragmentation maps are shown below the series of spectra. The m/z values of the fragment ions in C (UVPD) are summarized in Supplemental Table 1. The pound sign (#) indicates the loss of CO_2.

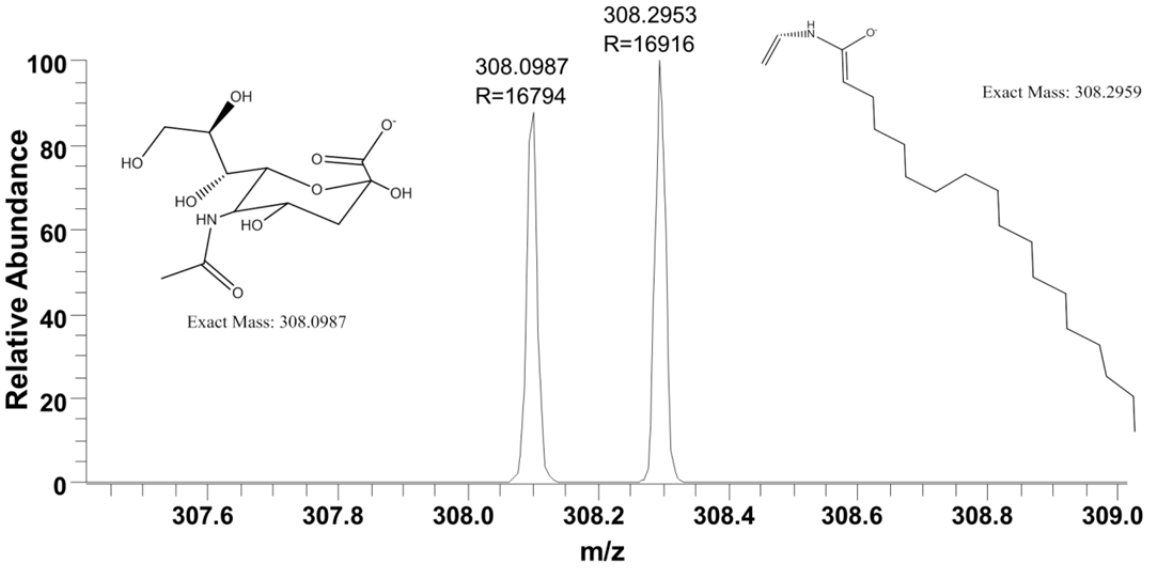

Supplemental Figure 7. Expanded region of HCD mass spectrum of singly charged GD1a(18:1/18:0) with the corresponding structures of the fragment ions.

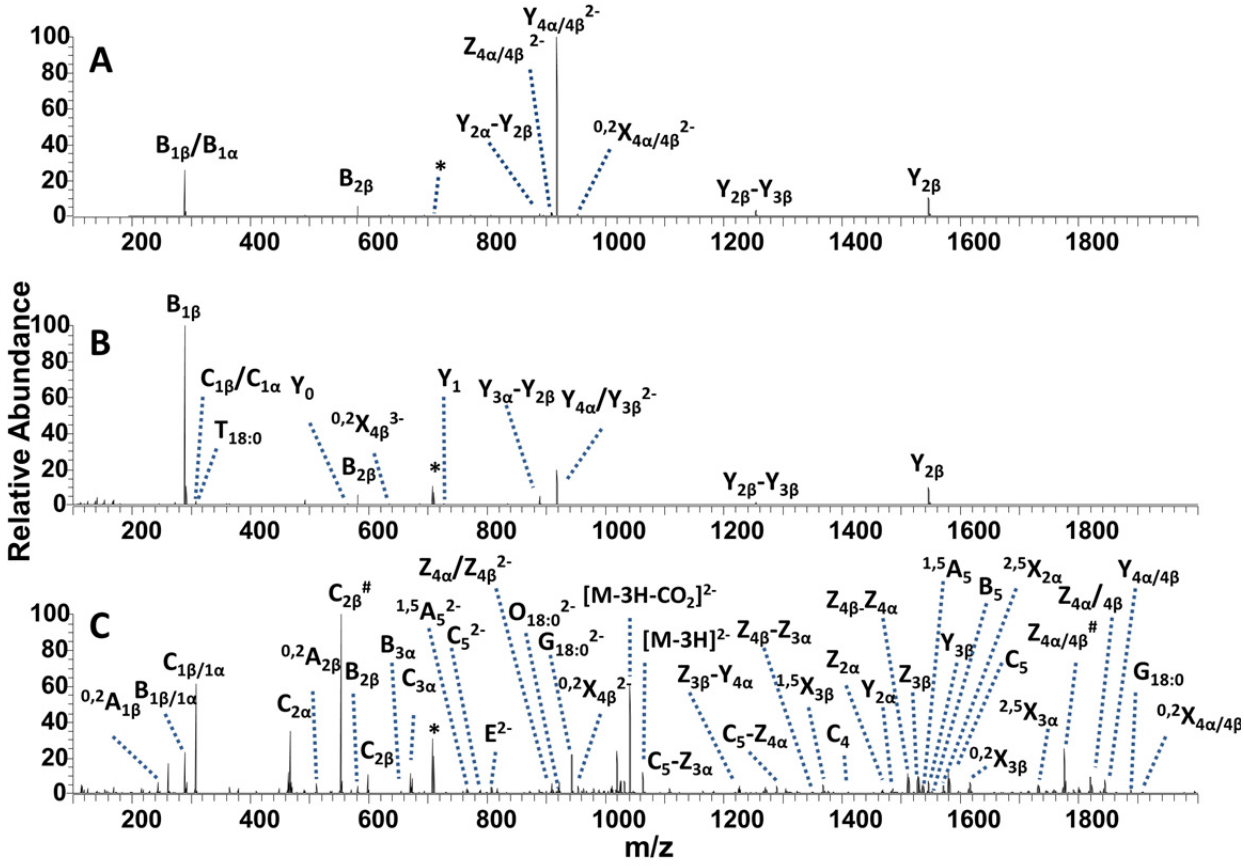

Supplemental Figure 8. (A) CID, (B) HCD and (C) UVPD mass spectra of the triply deprotonated porcine brain ganglioside GT1b(18:1/18:0). The precursor ion is labelled with an asterisk. The pound sign (#) indicates the loss of CO_2.

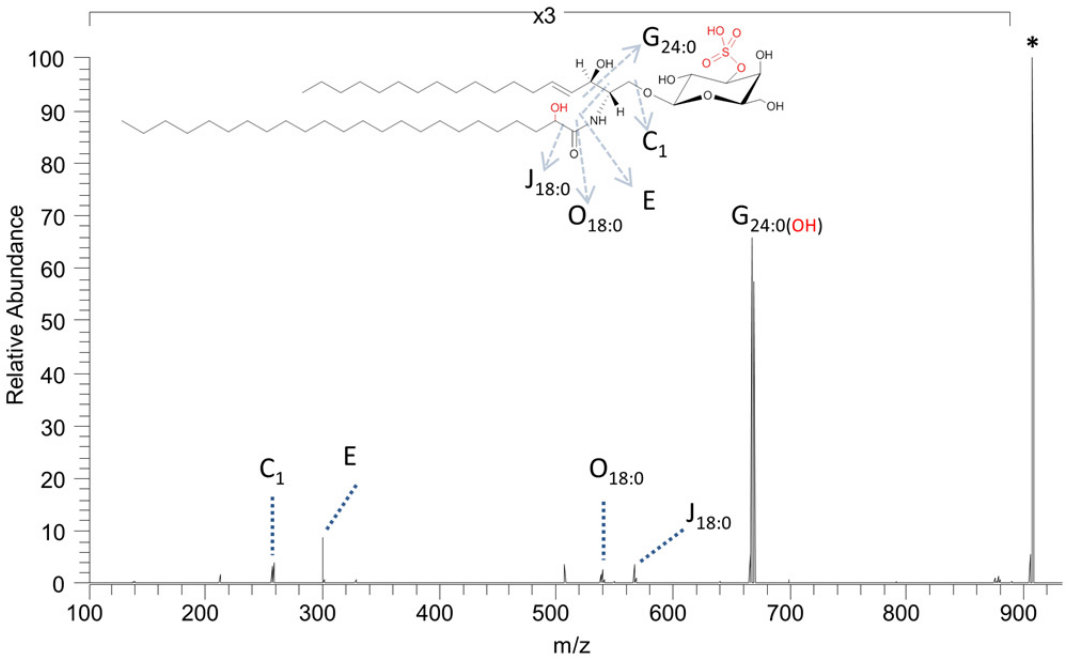

Supplemental Figure 9. LC-UVPD mass spectrum of singly charged (3'-sulfo)Galβ-Cer(d18:1/24:0(2OH)) obtained from a porcine brain extract.

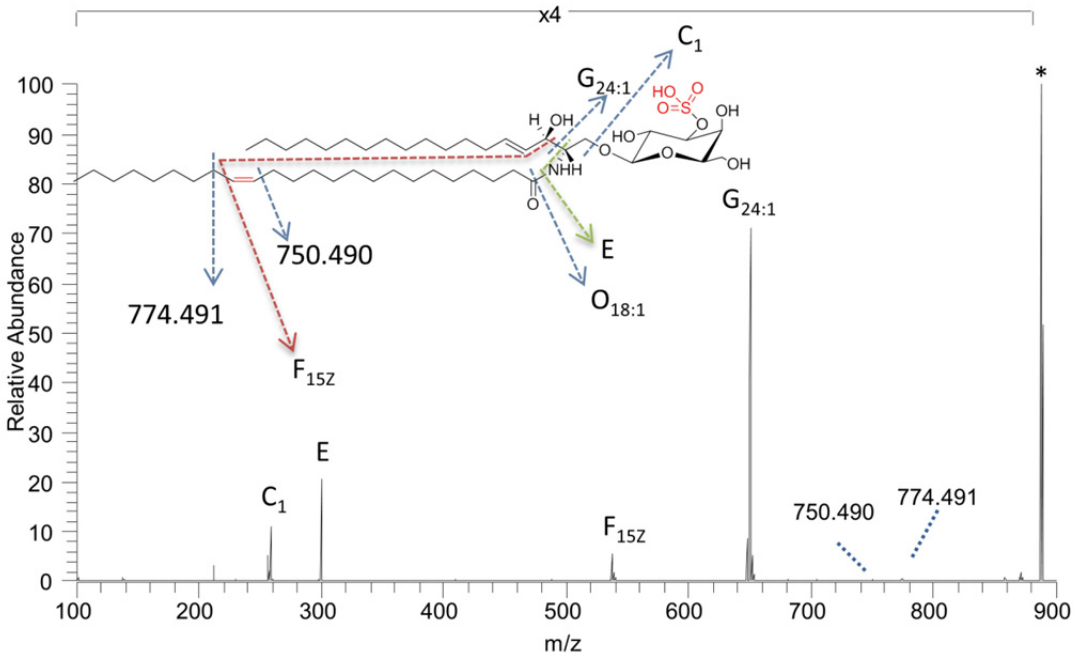

Supplemental Figure 10. LC-UVPD mass spectrum of singly deprotonated (3'-sulfo)Galβ-Cer(d18:1/24:1(15Z)) obtained from a porcine brain extract.

		[M-H]$^-$		[M-2H]$^{2-}$		
Fragment Ion	Expected Exact Mass	Observed m/z	error (ppm)	Observed m/z	error (ppm)	H-Migration
Ceramide Fragment ions						
E	673.231	673.231	0.0	673.23	-1.5	
$O_{17:1}$	897.446	897.446	0.0	897.446	0.0	
$O_{18:1}$	911.462	911.461	-1.1	911.459	-3.3	
$O_{19:1}$	925.477	925.476	-1.1	925.469	-8.6	
$G_{22:0}$	997.570	997.571	1.0	995.553	-1.4	- H_2
$G_{23:0}$	1011.586	1011.586	0.0	1009.568	-2.4	- H_2
$G_{24:0}$	1025.601	1025.602	0.6	1023.583	-2.7	- H_2
Cross-Ring Fragment ions						
$^{0,2}A_1$	220.083	220.083	0.0	220.082	-4.5	
$^{0,2}A_2$	408.116	408.115	-2.5	408.114	-4.9	
$^{1,5}A_2$	426.162	426.162	0.0	426.161	-2.3	
$^{2,4}A_3$	512.163	512.163	-0.4	513.169	-3.9	+ H
$^{3,5}A_3$	526.179	526.178	-1.9	526.177	-3.8	
$^{0,2}A_3$	570.169	570.168	-1.8	570.167	-3.5	
$^{1,5}A_3$	588.215	588.215	0.0	588.214	-1.7	
$^{0,2}X_2$	1028.726	1028.726	0.0	1028.724	-1.9	
$^{3,5}X_2$	1075.739	1075.738	-0.9	1074.727	-3.9	- H
Glycosidic Fragment ions						
B_1	290.088	290.089	3.4	290.088	0.0	
C_1	308.099	308.099	0.0	308.098	-3.2	
B_2	451.134	451.133	-2.2	451.133	-2.2	
C_2	468.137	468.136	-2.1	468.135	-4.3	
B_3	613.187	613.186	-1.6	613.185	-3.3	
C_3	632.204	632.205	1.6	632.203	-1.6	
Z_1	778.657	778.656	-1.3	778.654	-3.9	
Y_1	796.667	796.668	1.3	796.669	2.5	
Z_2	938.694	938.694	0.0	938.692	-2.1	
Y_2	958.720	958.721	1.0	958.718	-2.1	
Neutral Loss Product Ions						
[M-C2H6O2-H]$^-$	1187.778	1187.775	-2.9	1187.78	1.3	
[M-H-CO2]-	1205.825	1205.826	0.5	1205.812	-11.1	

Supplemental Table 1. UVPD fragment ions for singly deprotonated and doubly deprotonated ganglioside GM3 from Figure 3C and Supplemental Figure 6C.

Identified Species	G/O Pairs	Observed m/z	Ion Charge	Theoretical m/z	Error (ppm)
GQ1 Gangliosides					
GQ1b(18:1/20:0)	$G_{20:0}/O_{18:1}$	814.729	3-	814.724	-6.1
GQ1b(18:1/22:0)	$G_{22:0}/O_{18:1}$	824.068	3-	824.072	-4.9
GT1 Gangliosides					
acyl-GT1b(d18:1/20:0)	$G_{20:0}/O_{18:1}$	731.701	3-	731.696	-6.8
GT1b(18:1/18:0)	$G_{18:0}/O_{18:1}$	708.353	3-	708.349	-5.6
GT1b(18:1/20:0)	$G_{20:0}/O_{18:1}$	717.698	3-	717.692	-8.4
GT1b(18:1/21:0)	$G_{21:0}/O_{18:1}$	722.358	3-	722.352	-8.3
GT1b(18:1/22:0)	$G_{22:0}/O_{18:1}$	727.041	3-	727.036	-6.9
GD1 Gangliosides					
acyl-GD1b(d18:1/16:0)	$G_{16:0}/O_{18:1}$	924.474	2-	924.468	-6.5
GD1a(18:1/18:0)*	$G_{18:0}/O_{18:1}$	917.487	2-	917.479	-8.7
GD1b(18:1/18:0)*	$G_{18:0}/O_{18:1}$	917.487	2-	917.479	-8.7
GD1a(18:1/19:0)*	$G_{19:0}/O_{18:1}$	924.474	2-	924.468	-6.5
GD1a(19:1/18:0)*	$G_{18:0}/O_{19:1}$	924.474	2-	924.468	-6.5
GD1a(18:1/20:0)*	$G_{20:0}/O_{18:1}$	931.490	2-	931.494	4.3
GD1b(18:1/20:0)*	$G_{20:0}/O_{18:1}$	931.490	2-	931.494	4.3
GD1a(20:1/18:0)*	$G_{18:0}/O_{20:1}$	931.490	2-	931.494	4.3
GD1b(20:1/18:0)*	$G_{18:0}/O_{20:1}$	931.490	2-	931.494	4.3
GalNAcβ1-4(NeuAcα2-3)Galβ1-3GalNAcβ1-4(NeuAcα2-3)Galβ1-4Glcβ-Cer(d18:1/18:0)	$G_{18:0}/O_{18:1}$	1019.025	2-	1019.019	-5.9
Fucα1-2Galβ1-3GalNAcβ1-4(NeuAcα2-8NeuAcα2-3)Galβ1-4Glcβ-Cer(d18:1/18:0)	$G_{18:0}/O_{18:1}$	990.514	2-	990.508	-6.1
GalNAcβ1-4(NeuAcα2-3)Galβ1-3GalNAcβ1-4(NeuAcα2-3)Galβ1-4Glcβ-Cer(d18:1/20:0)	$G_{20:0}/O_{18:1}$	1033.042	2-	1033.034	-7.7
GD3 Gangliosides					
acyl-GD3(d18:1/18:0)	$G_{18:0}/O_{18:1}$	1512.852	1-	1512.843	-5.9
GD3(d18:1/18:0)	$G_{18:0}/O_{18:1}$	1470.841	1-	1470.833	-5.4
GM1 Gangliosides					
GM1a(18:1/16:0)	$G_{16:0}/O_{18:1}$	1516.845	1-	1516.838	-4.6
GM1a(18:1/18:0)	$G_{18:0}/O_{18:1}$	1544.878	1-	1544.869	-5.8
GM1a(18:1/20:0)*	$G_{20:0}/O_{18:1}$	1572.911	1-	1572.901	-6.4
GM1a(20:1/18:0)*	$G_{18:0}/O_{20:1}$	1572.911	1-	1572.901	-6.4
Fucα1-2Galβ1-3GalNAcβ1-4(NeuAcα2-3)Galβ1-4Glcβ-Cer(d20:1/18:0)*	$G_{18:0}/O_{20:1}$	1718.967	1-	1718.959	-4.7
Fucα1-2Galβ1-3GalNAcβ1-4(NeuAcα2-3)Galβ1-4Glcβ-Cer(d18:1/20:0)*	$G_{20:0}/O_{18:1}$	1718.967	1-	1718.959	-4.7

Supplemental Table 2. Major porcine gangliosides identified via LC-UVPD-MS corresponding to the chromatogram in Figure 5. Gangliosides labelled with an asterisk indicate that the specific species was elucidated by UVPD for co-eluting species

Sulfotide Species	Fragment Ion Series	Observed m/z	Ion Charge	Theoretical m/z	Error (ppm)
(3'-sulfo)Galβ-Cer(d18:1/20:0)	$G_{20:0}/O_{18:1}$	834.583	1-	834.577	-7.2
(3'-sulfo)Galβ-Cer(d18:1/24:1(15Z))	$G_{24:1}/O_{18:1}/K_{15Z}$	888.63	1-	888.624	-6.8
(3'-sulfo)Galβ-Cer(d18:0/24:0(2OH))	$G_{24:0}/O_{18:1}/J_{18:0}$	906.641	1-	906.635	-6.6

Supplemental Table 3. Porcine sulfotides identified via LC-UVPD-MS corresponding to the chromatogram in Figure 5.